A Technique to Enhance Localization in the Presence of NLOS Errors

Satyajayant Misra, Weiyi Zhang and Guoliang Xue†

***Abstract*— In a wireless network (WN), the wireless devices generally localize themselves with the help of anchors that are pre-deployed in the network. Some of the techniques commonly used for localization are Time of Arrival (ToA), Time Difference of Arrival (TDoA), Angle of Arrival (AoA), and Time of Flight (ToF). In the wireless domain, measurements are susceptible to errors resulting from the nature of the medium, the relatively low precision, and the presence of obstacles, which produce Non-Line Of Sight (NLOS) errors. The NLOS errors are a major concern as they could result in significant degradation in accuracy. In this paper, we propose an efficient technique that uses the distance estimates of the device from a group of anchors to localize the device with better accuracy in the presence of NLOS errors. Our technique is based on the notion that in general, for any estimate, the proportion of the NLOS error can be upper bounded. Using this upper bound information our technique reduces the uncertainty in the position of the wireless device that is being localized. The technique is distributed and is simple. In comparison to the standard localization procedure, where localization is done independent of the presence of NLOS errors, our technique uses the information about the NLOS error bounds to improve the accuracy of estimation. Simulation results show that our technique reduces the position error of the wireless device by 40% on an average and by at least 80% in the best case. The uncertainty in localization is also reduced significantly.**

I. Introduction

Large scale distributed wireless networks (WNs) have become popular in both the military and civilian domains [1]. Despite significant improvements in the abilities of these networks, there still exist many fundamental problems that need to be addressed.The problem of robust localization of the wireless nodes is one such fundamental problem in a WN. In a infrastructureless wireless network (IWN), accurate localization is very important as most applications require the position of the data source to utilize the data better. In the infrastructure-based network (IBWN) or the cellular networks, localization is useful to provide services, such as 911 call location identification. In an IWN, for cost effectiveness most nodes localize themselves using their position estimates obtained from a group of nodes in the network called the *anchors* [12], [13]. In the IBWN, the basestations (BSs) perform the same role. The anchors/BSs are fixed wireless nodes that know their own positions accurately, either through GPS or from pre-programmed information. In this paper, we use the term *anchor* to refer to both the anchor (in IWN) and the basestation (in IBWN).

In WNs the problem of accurate localization is fairly complex due to the inherent errors in measurements resulting from barriers, such as transmission delay and interference. In addition, WNs also suffer from the Non-Line Of Sight (NLOS) errors. NLOS errors result from obstacles between the wireless device (WD) and the anchors, which result in the dilation of the estimates of the device's position obtained by each anchor. The NLOS errors result in significant inaccuracies in measurement and are difficult to identify. In what follows, we illustrate the extent of inaccuracy that can result from NLOS errors.

In a WN, there are generally two possible mechanisms for localization, range-based and range-free [9]. In this paper, we study only range-based localization, with attention to the Time of Arrival (ToA) [13], [14] based technique. For exposition, we assume that the location estimation happens at the WD itself. Our technique also supports the alternate mechanism where a centralized agent performs localization. Following the ToA method, each anchor a_i periodically broadcasts its identifier (ID) and position information in its neighborhood, as a radio signal (RS) and an ultrasound signal (US) at the same instance of time. We denote these two components together as the *location reference*. On receipt of the location reference l_i from a_i, each WD u, calculates the time difference in receipt of the signals and uses the constants, speed of light (c) and sound (s), to obtain an estimate $\hat{r}_i$ of its distance (r_i) from a_i. The calculation of the estimate $\hat{r}_i$ is given below by Equations 1 and 2 as,

$$\Delta t = \hat{r}_i/s - \hat{r}_i/c, \tag{1}$$

$$\hat{r}_i = \Delta t \cdot \frac{1}{1/s - 1/c}, \tag{2}$$

where Δt refers to the difference in time between the receipt of the RS and the US. Due to errors during transmission, the value of Δt is inaccurate. This results in u being able to only estimate r_i. When u gets a sufficient number of location references from anchors in its range it uses them to estimate its own position ($\mathbf{u}$). The estimation can be done using techniques based on the Minimum Squared Error (MSE) method ([14]), the maximum likelihood method ([4]), or convex optimization ([7], [12]).

Given a WD u, we define the *bound circle* (C_i) of an anchor a_i in its range, as the circle with a_i's position as the center and the radius equal to the estimate of the distance

This research was supported in part by ARO grant W911NF-04-1-0385 and NSF grants CNS-0524736 and CCF-0431167. The information reported here does not reflect the position or the policy of the federal government.

† All three authors are with the Department of Computer Science and Engineering, Arizona State University, Tempe, AZ 85287-8809. Email: {satyajayant, weiyi.zhang, xue}@asu.edu.

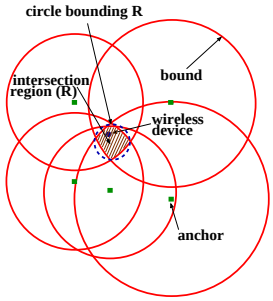

Fig. 1. Bound circles intersection (measurement errors present)

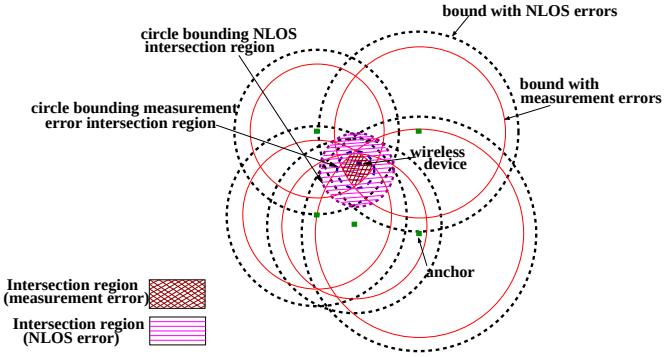

Fig. 2. Bound circles intersection (NLOS errors present)

between a_i and u. In the absence of any measurement errors, the position of u is the point of intersection of the bound circles corresponding to all the anchors in its range. However, when measurement errors exist, the intersection is no longer a point. *Positive errors* result in the distance estimate being greater than the true distance, while *negative errors* result in the estimate being lesser than the true distance. In the presence of positive errors, the intersection of the bound circles could result in a bounded intersection region $\mathcal{R}$, as shown in Fig. 1. Whereas, in the event of negative errors the intersection region may be empty (ϕ). In either case, it is difficult to identify the position of the WD accurately. NLOS errors result in a positive bias in the estimates and are generally bigger than the positive measurement errors. Hence, in the presence of NLOS errors with or without positive measurement errors, invariably $\mathcal{R}$ is significantly larger than that obtained with only positive measurement errors. This difference is illustrated in Fig. 2. The dashed circles are the bounds obtained when the measurement is subjected to NLOS errors, while the solid circles represent the bounds resulting from only positive measurement errors (no NLOS errors). The brown cross-hatched area represents the intersection region obtained from the bound circles with measurement errors, and the pink horizontal-hatched area represents the intersection region obtained from the bound circles with NLOS errors. The increase in the size of the intersection region due to NLOS errors in easily discernible. The bigger intersection region significantly increases the uncertainty in the estimation of the WD's position. In the presence of positive measurement errors and NLOS errors, the intersection region $\mathcal{R}$ can be approximated by the smallest circle that encloses it, as shown in Figs. 1 and 2. The position of the WD can be approximated as the center of this circle [12]. In the presence of negative measurement errors, the bound circles can be increased to obtain an $\mathcal{R}$ within which the WD is certain to exist.

In this paper, we denote the proportion of measurement error, for an anchor a_i, as $\delta_i \in [-\delta_{max}, \delta_{max}]$, and the NLOS error as, $\epsilon_i \in [0, \epsilon_{max}]$. If the true distance from a_i to the WD u is given by r_i, in the presence of measurement errors, the estimated distance is, $\hat{r}_{i\delta} = r_i \cdot (1 + \delta_i)$. If the measurement is subjected to NLOS error then the resultant distance estimate is, $\hat{r}_{i\epsilon} = r_i \cdot (1 + \delta) \cdot (1 + \epsilon_i)$. The values of δ_i and ϵ_i are unknown. This lack of information makes it difficult to obtain r_i from $\hat{r}_{i\epsilon}$. In addition, the NLOS errors result in significant increase in $\mathcal{R}$ and consequently, greater inaccuracy in localization.

We propose a technique that reduces the inaccuracies in estimation of the position of the WD in the presence of NLOS measurements by reducing the size of $\mathcal{R}$. It is efficient and requires inexpensive computations, easily afforded by the low power WDs. Simulation results demonstrate the efficacy of our technique. The size of $\mathcal{R}$ is reduced by at least 25% on an average and by more than 90% in the best case. The error in estimation of the position of the WD is reduced by at least 40% on an average and by atleast 80% in the best case.

In Section II, we present the related work. In Section III, we present the system model along with our assumptions. Section IV presents our proposed technique, while Section V presents the simulation results. We conclude our paper in Section VI.

II. Related Work

ToA and TDoA are the most popular schemes used for range-based localization in wireless networks. These schemes are non-linear and are generally solved by linearization and gradient search [8].The effectiveness of these schemes depends on the choice of the starting point and they are also not guaranteed to converge. Improvements to the schemes have resulted in closed form linear techniques that give optimal location estimates but at high SNR values [3]. There are several mechanisms for NLOS error mitigation [5]. One of them is the use of matched field processing based on scattering models [2], however, the scattering models are not accurate nor dynamic. Another mechanism is localization using both the LOS and NLOS measurements, with the NLOS measurements weighted so as to reduce their contribution in localization [6], [10]. Although these schemes are guaranteed to work always, they are highly unreliable. LOS reconstruction is another mechanism, which requires the knowledge of deployment geometry, error statistics, and timing history [15]. Another mechanism is identification of LOS measurements from all

the NLOS measurements and using only the LOS measurements for localization [5]. The identification can be performed using probabilistic models and time-history based hypothesis tests. This mechanism suffers from inaccurate identification of the LOS measurements and needs atleast 3 LOS measurements.

All the schemes mentioned above require expensive computations and a powerful centralized agent to perform the compute intensive calculations. These schemes cannot be utilized by current generation wireless devices for accurate localization in a NLOS environment. In this paper, we propose a distributed technique that is simple and efficient and can be easily implemented in the low power WDs for performing accurate localization in a NLOS setting. We compare the efficiency of our technique with the standard localization technique. We intend to pursue detailed comparison with other existing schemes as future work.

III. System Model and Assumptions

The system model and assumptions for our proposed technique are given below:

- The network consists of a set of anchors $\mathcal{A} = \{a_i, i = 1, \ldots, N\}$ that are deployed randomly and are fixed after deployment.
- The devices (WDs) being localized may be static or mobile.
- Each anchor a_i knows its own position $\mathbf{a_i}$ ($\mathbf{a_i} = (a_{ix}, a_{iy})$).
- The transmission range of the WDs is r and that of the anchors is R ($R \geq r > 0$).
- The measurement error proportion of anchor a_i is given by, $\delta_i \sim$ U$[-\delta_{max}, \delta_{max}]$.
- The NLOS error proportion of anchor a_i is, $\epsilon_i \sim$ U$[0, \epsilon_{max}]$, where ϵ_{max} is a system parameter. We note that often ϵ_{max} can be bounded with the knowledge of the anchors deployment layout, terrain geometry, and the environment [10], [15].
- All devices have omnidirectional antennas.

IV. Description of the Technique

We have noted earlier that in the presence of positive measurement errors and/or NLOS errors (with/without measurement errors) the actual position of the WD exists inside the intersection region ($\mathcal{R}$). That is, if P_i is the set of points inside the bound circle of anchor $a_i (i = 1, \ldots n)$, in the range of the WD, then the region $\mathcal{R} = \{x | x \in \mathbf{R}^2, x \in \cap_{i=1}^{n} P_i\}$. Since we make no assumption regarding the distribution of the distance estimates all points inside the region $\mathcal{R}$ are equally likely to be the position of the WD. When the measurement errors are negative there might not be an intersection region. To handle this scenario, the bounds of the anchors can be increased proportional to δ_{max} ($\hat{r}_{i\epsilon} = \hat{r}_{i\epsilon} \cdot (1 + \delta_{max})$). This would result in an intersection region containing the WD inside it. This procedure increases the size of $\mathcal{R}$, in general. However, we contend that the increase shall be small compared with that due to NLOS errors, with minimal effect on localization accuracy.

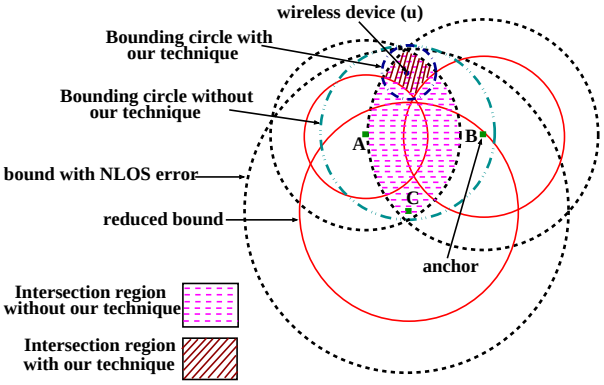

Fig. 3. Reduction in $\mathcal{R}$ resulting from the reduced bounds

Given the region ($\mathcal{R}$), it can be enclosed by a circle (C_B) [12]. C_B is referred to as the *enclosing circle*. The center of C_B can be obtained using convex optimization [12] and the position of the WD can be approximated by the center of C_B. The use of the center as an approximation of the WD's position minimizes both the average and worst case errors [12]. In this paper, we present another simpler technique that uses the points of intersection of the bound circles. Some of these points form the vertices of $\mathcal{R}$. Using these vertices the smallest circle (C_B) that encloses $\mathcal{R}$ can be obtained. The technique is described below.

Finding the smallest enclosing circle of $\mathcal{R}$: The intersection region $\mathcal{R}$ can be defined by the vertices of $\mathcal{R}$. In most cases, the smallest circle enclosing all the vertices of $\mathcal{R}$ also encloses $\mathcal{R}$. However, there are some cases where this is not true. We describe how to handle these cases in Algorithm 1. We note that reduction of $\mathcal{R}$ can improve the localization accuracy significantly. To reduce $\mathcal{R}$, we use the fact that given an anchor a_i and its estimated bound $\hat{r}_{i\epsilon}$ for a WD u, we can reduce the bound of a_i to $\hat{r}'_{i\epsilon}$, where,

$$\hat{r}'_{i\epsilon} = \hat{r}_{i\epsilon} / \{(1 + \delta_{max}) \cdot (1 + \epsilon_{max})\}, \quad (3)$$

such that $\mathbf{u} \notin C'_i$, the reduced bound circle with radius $\hat{r}'_{i\epsilon}$, centered at $\mathbf{a_i}$. We note that $\mathbf{u} \notin C'_i$ implies that $\| \mathbf{u} - \mathbf{a_i} \| \geq \hat{r}'_{i\epsilon}$. Applying this procedure for each anchor a_i in the range of u results in a C'_i for each a_i. Let $P'_i = \{x | \ \| x - \mathbf{a_i} \| < \hat{r}'_{i\epsilon}\}$, consequently $\mathcal{R}$ is reduced to, $\mathcal{R} = \{x | x \in \mathbf{R}^2, x \in \{\cap_{i=1}^{n} P_i \setminus \cup_{i=1}^{n} P'_i\}\}$, as illustrated in Fig. 3. In the figure, A, B, and C are three anchors in the range of the WD u. The dotted circles represent the bound circles obtained using the distance estimates from A, B, and C. The intersection region $\mathcal{R}'$ resulting from the intersection of these bound circles is the dash-hatched pink area. The solid red circles are the reduced bound circles of A, B, and C obtained using Equation 3. The reduced intersection area $\mathcal{R}$ is the solid-hatched brown area. Hence the C'_is result

in a reduction in the intersection region, thus reducing the uncertainty in localizing the WD. As shown in the figure, the enclosing circle obtained when our technique is used is significantly smaller than that obtained otherwise. This illustrates the effectiveness of our technique.

Algorithm 1 Algorithm for reducing the size of $\mathcal{R}$

1: INPUTS: Position $\mathbf{a_i}$ of the anchors in range of the WD and their estimates $\hat{r}_{i\epsilon}, i = 1, \ldots, n$.
2: OUTPUTS: $\mathbf{C_B}(x_B, y_B, r_B)$, the enclosing circle of $\mathcal{R}$;
3: **for** $i = 1$ to n **do**
4: $\hat{r}'_{i\epsilon} = \hat{r}_{i\epsilon}/\{(1+\delta_{max})(1+\epsilon_{max})\}$; {Reduced bound circles}.
$\hat{r}_{i\epsilon} = \hat{r}_{i\epsilon} \cdot (1+\delta_{max})$; {Ensures $\mathcal{R} \neq \phi$}.
5: **end for**
6: INITIALIZATION: $\mathbf{C} = \{C_i(x_i, y_i, \hat{r}_{i\epsilon})|\ C_i =$ bound circle of $a_i\}$; $\mathbf{C'} = \{C'_i(x_i, y_i, \hat{r}'_{i\epsilon})|\ C'_i =$ reduced bound circle of $a_i\}$, $i = 1, \ldots, n$.
7: OBTAIN: $\mathrm{V}_{CC} = \{\mathrm{x}|$ x is a point of intersection of $C_i, C_j \in \mathbf{C}\}$; $\mathrm{V}_{C'C'} = \{\mathrm{x}|$ x is a point of intersection of $C'_i, C'_j \in \mathbf{C'}\}$; $\mathrm{V}_{CC'} = \{\mathrm{x}|$ x is a point of intersection of $C_i \in \mathbf{C}, C'_j \in \mathbf{C}\}$; $i, j = 1, \ldots, n$.
8: $\mathrm{V}_{all} = \mathrm{V}_{CC} \cup \mathrm{V}_{C'C'} \cup \mathrm{V}_{CC'}$; {all intersection points}
9: $\mathrm{V} = \{\mathrm{x}|\ (\mathrm{x} \in V_{all}) \wedge (\mathrm{x} \in \cap_{i=1}^{n} C_i \setminus \cup_{i=1}^{n} C'_i\}$;
10: V' = ϕ;
11: $\mathbf{C}_{all} = \mathbf{C} \cup \mathbf{C'}$;
12: **for** each $C \in \mathbf{C}_{all}$ **do**
13: **for** each pair of intersection points (x_l, x_m) on C **do**
14: Bisect the chord formed by (x_l, x_m), the intersection points on C, by the perpendicular bisector from the center of C;
15: Extend the bisector to intersect C at points x_p and x_q;
16: **if** $\{\mathrm{x}_p \in \cap_{i=1}^{n} C_i \setminus \cup_{i=1}^{n} C'_i\}$ **then**
17: V' = V'$\cup\{\mathrm{x}_p\}$;
18: **end if**
19: **if** $\{\mathrm{x}_q \in \cap_{i=1}^{n} C_i \setminus \cup_{i=1}^{n} C'_i\}$ **then**
20: V' = V'$\cup\{\mathrm{x}_q\}$;
21: **end if**
22: **end for**
23: **end for**
24: V = V $\cup$ V';
25: Find the smallest circle $\mathbf{C_B}(\mathbf{x_B}, \mathbf{y_B}, \mathbf{r_B})$, such that $\| x - x_B \| \leq r_B\ \forall x \in$ V.
26: return $\mathbf{C_B}(x_B, y_B, r_B)$;

Algorithm 1 presents our technique. Lines **3** to **5** perform the reduction of the distance estimates to obtain the reduced bound circles and also the dilation of the distance estimates to ensure that negative errors do not result in $\mathcal{R} = \phi$. Line **6** performs the initialization of the sets **C** and **C'** that contain the bound circles and the reduced bound circles, respectively, of the anchors in range of the WD. Line **7** obtains the set of all intersection points of any pair of bound circles. Line **9** obtains V, the set that contains all the

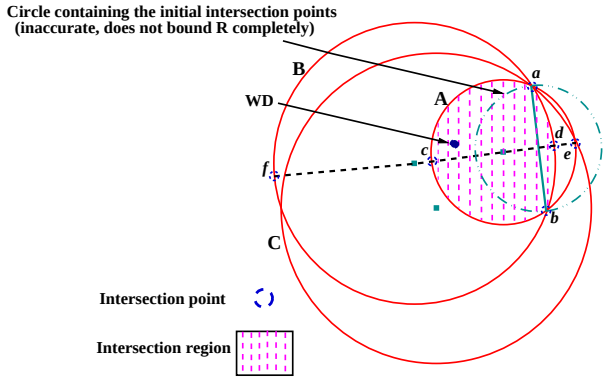

Fig. 4. Demonstration of need for extra intersection points

intersection points or vertices inside the intersection region $\mathcal{R}$. Lines **12** to **23** handle the special case where even though C_B contains all the vertices in $\mathcal{R}$ it is unable to enclose $\mathcal{R}$ completely. Fig. 4 provides an illustration of this special case. In the figure, there are three bound circles, A, B, and C. $V = \{a, b\}$, is the set of vertices of $\mathcal{R}$, with both A and B intersecting at the two points. However, the smallest circle containing both a and b (green circle in dot-dot-dash) does not enclose $\mathcal{R}$. This is because it bounds only the minor arc $\overset{\frown}{\mathrm{ab}}$ of B and not the major arc $\overset{\frown}{\mathrm{ab}}$ of A, which are the two bounding arcs of $\mathcal{R}$, and hence does not enclose $\mathcal{R}$ completely. It is easy to see that the smallest circle that contains all the bounding arcs of the region $\mathcal{R}$ (minor $\overset{\frown}{\mathrm{ab}}$ of B and major $\overset{\frown}{\mathrm{ab}}$ of A in this instance), encloses $\mathcal{R}$ as well. To make sure all the arcs bounding $\mathcal{R}$ are contained inside the smallest enclosing circle, lines **12** to **23** add to V, all the center points of the arcs, obtained using the end points of the arcs, that is, the vertices of $\mathcal{R}$. For instance, in Fig. 4 points d and c are added as follows. Line $\overline{fe}$ is the perpendicular bisector of the chord $\overline{ab}$. $\overline{fe}$ intersects the minor arc $\overset{\frown}{\mathrm{ab}}$ of B at d and the major arc $\overset{\frown}{\mathrm{ab}}$ of A at c. Thus, due to $\overline{fe}$ the set V becomes $V = \{a, b, c, d\}$, and the set of arcs becomes, $\mathcal{S} = \{\overset{\frown}{\mathrm{ac}}, \overset{\frown}{\mathrm{cb}}, \overset{\frown}{\mathrm{bd}}, \overset{\frown}{\mathrm{da}}\}$; set $\mathcal{S}$ will never contain a major arc. We note here that the radius (r_B) of the smallest circle (C_B) enclosing $\mathcal{R}$ satisfies the inequality, $r_B \leq \min\{\hat{r}_{i\epsilon}, i = 1, \ldots, n\}$.This is because the smallest bound circle encloses $\mathcal{R}$ also. In the figure, the smallest circle that contains V is circle A, hence using Lemma 1, we can say that A also contains $\mathcal{S}$ ($\mathcal{S} \in A$), and is the enclosing circle C_B of $\mathcal{R}$. If $\mathcal{S} \notin C_B$, then there exists an arc $\{\overset{\frown}{\mathrm{xy}}|\ (\overset{\frown}{\mathrm{xy}} \in \mathcal{S}) \wedge (\overset{\frown}{\mathrm{xy}} \notin C_B)\}$. Let $\overset{\frown}{\mathrm{xy}}$ be a part of a bound circle C_X, then $\overset{\frown}{\mathrm{xy}}_X > \overset{\frown}{\mathrm{xy}}_B$, hence $r_B > r_X$ from Lemma 1, where r_B is the radius of C_B and r_X the radius of C_X. This contradicts the condition, $r_B \leq \min\{\hat{r}_{i\epsilon}, i = 1, \ldots, n\}$, hence $\mathcal{S} \in C_B$. If points x and y are inside C_B, then Lemma 1 still applies to the arc formed by the points of intersection of $\overset{\frown}{\mathrm{xy}}$ with C_B.

Lemma 1: Let two circles C_1 and C_2 with radius r_1 and r_2 respectively, intersect at two points p and q. Let the minor arc corresponding to C_1 be $\overset{\frown}{\mathrm{pq}}_1$ and that corresponding to

C_2 be $\widehat{pq}_2$. If $\widehat{pq}_1 \geq \widehat{pq}_2$, then $r_1 \leq r_2$. Also if $r_1 \geq r_2$, then $\widehat{pq}_1 \leq \widehat{pq}_2$.

Proof: We will prove this by contradiction. Let us assume that $r_1 > r_2$, then the line C_1C_2 joining the centers of C_1 and C_2 and bisecting chord pq intersects C_2 at two points, say l and m, where m is the point on the major arc $\widehat{pq}_2$. m should be inside C_1 as $r_1 > r_2$. This implies that C_2 intersects C_1 at 4 non-collinear points (p and q being 2 of them). According to the properties of circles, only one unique circle can pass through three or more non-collinear points. Thus C_1 and C_2 are the same circle, this implies that $r_1 = r_2$, which is a contradiction. Thus we prove that $r_1 \leq r_2$. Since $\widehat{pq}_1 \geq \widehat{pq}_2$, thus $\widehat{pq}_2 \in C_1$. Using negation, $\sim (\widehat{pq}_1 \geq \widehat{pq}_2 \implies r_1 \leq r_2)$, we have, $r_1 \geq r_2 \implies \widehat{pq}_1 \leq \widehat{pq}_2$. ■

Line **25** finds the smallest circle that encloses $\mathcal{R}$ and hence the set V within it. The center (x_B, y_B) is the estimate of the WD's position, while C_B is the uncertainty region, with r_B being its radius. Theorem 1 proves that in the worst case the size of the enclosing circle obtained by our technique is as big as that obtained when our technique is not used.

Theorem 1: Let $\mathcal{R}'$ be the region of intersection of the bound circles and $\mathcal{R}$ the region of intersection when the reduced bound circles are also used in localization. If r_B is the radius of the smallest circle (C_B) enclosing $\mathcal{R}$ and r'_B is the radius of the smallest circle (C'_B) enclosing $\mathcal{R}'$, then $r_B \leq r'_B$.

Proof: Let $P_i = \{x| \parallel x - \mathbf{a_i} \parallel \leq \hat{r}_{i\epsilon}\}$, where $\hat{r}_{i\epsilon}$ is the bound circle of a_i and $P'_i = \{x| \parallel x - \mathbf{a_i} \parallel < \hat{r}'_{i\epsilon}\}$ where $\hat{r}'_{i\epsilon}$ is the reduced bound circle of a_i, then $\mathcal{R}' = \{x | x \in \mathbf{R}^2, x \in \cap_{i=1}^{n} P_i\}$ and $\mathcal{R} = \{x | x \in \mathbf{R}^2, x \in \{\cap_{i=1}^{n} P_i \setminus \cup_{i=1}^{n} P'_i\}\}$, so $\mathcal{R} \subseteq \mathcal{R}'$. Thus, C'_B also bounds $\mathcal{R}$, hence $r_B \leq r'_B$. ■

The running time of line **7** of Algorithm 1 is $\mathcal{O}(3n^2)$, where n is the number of anchors in range of the WD. Running time of line **8** is $\mathcal{O}(3n^2)$, of line **9** is $\mathcal{O}(2n^3)$, and of lines **12** to **23** is $\mathcal{O}(n^2)$. The smallest circle enclosing $\mathcal{R}$ can be obtained using the prune and search technique proposed by Nimrod Megiddo [11], hence the running time of line **25** is $\mathcal{O}(n^2)$. Hence the total running time of the algorithm is $\mathcal{O}(n^3)$.

V. Simulation Results

The WN is deployed in a square field of dimensions 100×100 m^2. A given number of anchors are deployed randomly in range of the WD, positioned at a random location in the network. The transmission range of the anchors is set to 30m and the location reference broadcast period is set to 1 second. The maximum error proportion was chosen to be $|\delta_{max}| = 0.1$, and the maximum NLOS error proportion was chosen as, $\epsilon_{max} \in [0.2, 0.6]$ for illustration. The value of δ_{max} is representative, while that of ϵ_{max} helps demonstrate the effectiveness of the scheme. The number of anchors (n) in range of the WD is between 3 to 7.

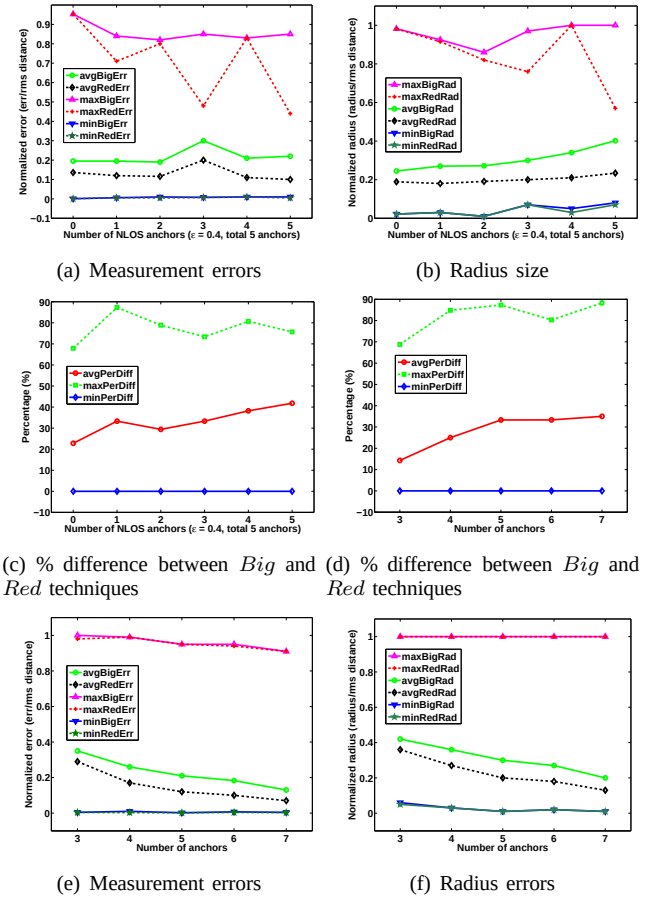

(a) Measurement errors (b) Radius size

(c) % difference between Big and Red techniques (d) % difference between Big and Red techniques

(e) Measurement errors (f) Radius errors

Fig. 5. 5(a), 5(b), and 5(c): Error, radius and percentage difference with different NLOS anchors given 5 anchors in range, $\epsilon = 0.4$. 5(d), 5(e) and 5(f): Percentage difference, error, and radius with different anchors in range, $\epsilon = 0.4$.

For each configuration of n, we vary the number of NLOS anchors from $0, \ldots, n$. For each configuration of ϵ, n, and number of NLOS anchors, we run the simulation for 50 runs and obtain the average, maximum, and minimum values of the performance parameters. We study two performance parameters: the measurement error (err), which is the error in estimating the true position of the WD by the center of the circle C_B enclosing $\mathcal{R}$, and the radius r_B of C_B. The measurements are normalized using the RMS distance value, $\hat{r} = \sqrt{(\frac{1}{n}\sum_{i=1}^{n} \hat{r}_{i\epsilon}^2)}$. In the figures, we refer to the standard technique that does not use the reduced circles as the Big, while our technique is referred to as the Red (reduced).

Fig. 5 illustrates some of the results of the simulations. In Fig. 5(a), we study the normalized error in measurement, given that some of the anchors, out of 5 anchors in range of the WD, are subjected to NLOS measurements. As can be seen the average normalized error when our technique is used is lesser than when localization is done using the standard technique. The error is reduced by 60% in the best case. Also, the error increases slowly in comparison to the Big technique. This is an encouraging result. The maximum and minimum errors also are no more than in the Big case.

TABLE I

RESULTS OF SIMULATION WITH ϵ

ϵ	Measurement Error (err)						Radius (r_B)						% Difference in radius		
	Average		Maximum		Minimum		Average		Maximum		Minimum		Average	Maximum	Minimum
	Big	Red	Big	Red	Big	Red	Big	Red	Big	Red	Big	Red			
0.2	0.178	0.091	0.99	0.99	0.0007	0.002	0.24	0.15	1.0	1.0	0.01	0.01	37.5	94.73	0.0
0.3	0.19	0.11	0.99	0.99	0.001	0.001	0.26	0.175	1.0	1.0	0.004	0.002	32.7	91.86	50.0
0.4	0.19	0.13	0.998	0.99	0.002	0.002	0.26	0.19	1.0	1.0	0.01	0.01	26.9	88.25	0.0
0.5	0.21	0.147	0.99	0.99	0.001	0.001	0.285	0.216	1.0	1.0	0.01	0.01	24.2	87.44	0.0
0.6	0.17	0.09	0.97	0.93	0.0008	0.0008	0.245	0.161	1.0	1.0	0.0086	0.0086	33.3	92.94	0.0

The cases where the maximum error of the Red technique correspond to the Big technique are those in which there is no reduction in $\mathcal{R}$ as a result of the reduced circles. Fig. 5(b) shows the maximum, minimum, and average normalized radius of C_B. Here as well, Red performs better than Big. Also the average normalized radius does not increase as fast as in the Big technique with increase in NLOS anchors and the maximum normalized radius in Red is no more than that in Big. Thus the average case performance of Red is better than Big while the worst case performance is no worse than Big. Fig. 5(c) shows the maximum, average, and minimum percentage difference between the radii obtained in the Big and Red techniques over 50 simulation runs. For all NLOS anchors configuration the normalized radius obtained by Red is at least 70% lesser than the radius obtained by Big in the best case, illustrated as maxPerDiff. In the average case the decrease is anywhere between 20% to 42%, with the percentage increasing with increase in NLOS anchors, which is a desirable property.

In Figs. 5(d)–5(f) we compare the performance of Big to Red for a different number of anchors. The results are taken over all configurations of NLOS anchors for each value of n. Fig. 5(d) shows the percentage difference between the radii obtained in the Red and Big techniques. The difference increases with the increase in the number of anchors. This is because with the increase in number of anchors the number of reduced bound circles increases thus resulting in greater decrease in area. The radius and the measurement errors also decrease for the same reason, as illustrated in 5(e) and 5(f) respectively.

Table I illustrates the measurement error, radius r_B, and the percentage difference in r_B between Big and Red, for different values of the NLOS proportion ϵ. Our technique performs better than Big for all values of ϵ on an average case. r_B in Red is atleast 25% lesser than r_B in Big. In the best case, r_B is as atleast 87% lesser than r_B in Big. In the statistic of measurement error as well, on an average Red has 40% lesser error than Big, and at least 80% lesser error in the best case. The results demonstrate the effectiveness of our technique in reducing $\mathcal{R}$ and decreasing the estimation error. As the value of ϵ increases the performance of the Red scheme approaches that of the Big scheme as the reduction in $\mathcal{R}$ becomes less. After a certain value of ϵ, there will be no reduction in $\mathcal{R}$. As proved in Theorem 1, the performance of the Red will be the same as Big.

VI. CONCLUSIONS AND FUTURE WORK

In this paper, we have proposed a simple technique that improves the accuracy of localization in the presence of NLOS measurement errors. In the future, we would attempt to improve the performance of our algorithm by increasing the size of the pessimistically chosen reduced bounds and also compare our technique with other existing schemes to demonstrate its usefulness.

REFERENCES

[1] I. Akyildiz, W. Su, Y. Sankarasubramaniam, and E. Cayirci. Wireless sensor networks: A survey. *Computer Networks*, 38(4):393–422, 2002.

[2] S. Al-Jazzar and J. Caffery Jr. ML and Bayesian TOA location estimators for NLOS environments. pages 1178–1181, 2002.

[3] J. Caffery. A new approach to the geometry of TOA location. pages 24–28, 2000.

[4] Y-T. Chan, Y. Hang, and H. Ching. Exact and approximate maximum likelihood localization algorithms. *IEEE Transactions on Vehicular Technology*, 55(1):10–16, jan 2006.

[5] Y.-T. Chan, W.-Y. Tsui, H.-C. So, and P. Ching. Time of arrival based localization under NLOS conditions. *IEEE Transactions on Vehicular Technology (TVT)*, 55(1):17–24, 2006.

[6] P. Chen. A NLOS error mitigation algorithm in location estimation. 1999.

[7] L. Doherty, K. Pister, and L Ghaoui. Convex position estimation in wireless sensor networks. In *Proceedings of the IEEE INFOCOM*, pages 22–26, 2001.

[8] W. Foy. Position-location solutions by taylor-series estimation. *IEEE Transactions on Aerospace and Electronic Systems (AES)*, 12(2):187–194, 1976.

[9] Tian He, Chengdu Huang, Brian M. Blum, John A. Stankovic, and Tarek F. Abdelzaher. Range-free localization and its impact on large scale sensor networks. *Trans. on Embedded Computing Sys.*, 4(4):877–906, 2005.

[10] N. Khajehnouri and A. Sayed. A non-line-of-sight equalization scheme for wireless cellular location. In *Proceeding of the IEEE International conference on Acoustics, Speech, and Signal Processing (ICASSP)*, pages 549–552, 2003.

[11] N. Megiddo. Linear-time algorithms for linear programming in R^3 and related problems. *SIAM Journal on Computing*, 12(4):759–776, 1983.

[12] S. Misra, S. Bhardwaj, and G. Xue. ROSETTA: Robust and secure mobile target tracking in a wireless ad hoc environment. In *Proceeding of the Military Communications Conference (MILCOM)*, pages 1–7, 2006.

[13] D. Niculescu and B. Nath. Error characteristics of ad hoc positioning systems (APS). In *Proceeding of ACM MobiHoc*, 2004.

[14] A. Savvides, C. Hans, and M. Srivastava. Dynamic fi ne-grained localization in ad-hoc networks of sensors. In *Proceeding of ACM MobiCom*, pages 166–179, 2001.

[15] S. Venkatraman, J. Caffery Jr., and H.-R. You. Location using los range estimation in nlos environments. In *Proceeding of Vehicular Technology Conference (VTC)*, pages 856–860, 2002.